Apolipoprotein E4 Exaggerates Diabetic Dyslipidemia and Atherosclerosis in Mice Lacking the LDL Receptor

Lance A. Johnson, Jose M. Arbones-Mainar, Raymond G. Fox, Avani A. Pendse, Michael K. Altenburg, Hyung-Suk Kim, and Nobuyo Maeda

OBJECTIVE—We investigated the differential roles of apolipoprotein E (apoE) isoforms in modulating diabetic dyslipidemia—a potential cause of the increased cardiovascular disease risk of patients with diabetes.

RESEARCH DESIGN AND METHODS—Diabetes was induced using streptozotocin (STZ) in human apoE3 (E3) or human apoE4 (E4) mice deficient in the LDL receptor ($LDLR^{-/-}$).

RESULTS—Diabetic $E3LDLR^{-/-}$ and $E4LDLR^{-/-}$ mice have indistinguishable levels of plasma glucose and insulin. Despite this, diabetes increased VLDL triglycerides and LDL cholesterol in $E4LDLR^{-/-}$ mice twice as much as in $E3LDLR^{-/-}$ mice. Diabetic $E4LDLR^{-/-}$ mice had similar lipoprotein fractional catabolic rates compared with diabetic $E3LDLR^{-/-}$ mice but had larger hepatic fat stores and increased VLDL secretion. Diabetic $E4LDLR^{-/-}$ mice demonstrated a decreased reliance on lipid as an energy source based on indirect calorimetry. Lower phosphorylated acetyl-CoA carboxylase content and higher gene expression of fatty acid synthase in the liver indicated reduced fatty acid oxidation and increased fatty acid synthesis. $E4LDLR^{-/-}$ primary hepatocytes cultured in high glucose accumulated more intracellular lipid than $E3LDLR^{-/-}$ hepatocytes concomitant with a 60% reduction in fatty acid oxidation. Finally, the exaggerated dyslipidemia in diabetic $E4LDLR^{-/-}$ mice was accompanied by a dramatic increase in atherosclerosis.

CONCLUSIONS—ApoE4 causes severe dyslipidemia and atherosclerosis independent of its interaction with LDLR in a model of STZ-induced diabetes. ApoE4-expressing livers have reduced fatty acid oxidation, which contributes to the accumulation of tissue and plasma lipids. ***Diabetes*** **60:2285–2294, 2011**

Cardiovascular disease (CVD) caused by a worsening of atherosclerosis is an important complication of diabetes and is the leading cause of mortality among patients with diabetes (1). Patients with poorly managed type 1 diabetes or type 2 diabetes commonly have elevated VLDL triglycerides (TGs), a reduction of HDL cholesterol, and smaller, dense LDL. This common cluster of harmful changes in lipid metabolism is referred to as diabetic dyslipidemia (2).

Apolipoprotein E (apoE) is a small circulating protein associated predominantly with VLDL and HDL. It is the primary ligand for several lipoprotein receptors, making it a crucial component in the clearance of lipid from the circulation and a major determinant of plasma cholesterol and CVD risk (3). In humans, the *APOE* gene is polymorphic, resulting in production of three common isoforms: apoE2, apoE3, and apoE4. The apoE4 isoform is carried by more than a quarter (28%) of the U.S. population and is associated with higher LDL cholesterol and an increased risk of CVD (3). In addition to its well-established role in CVD, recent findings have implicated a role for apoE in glucose metabolism. Epidemiological studies have suggested that in certain populations, *APOE* genotype may influence plasma glucose and insulin levels (4,5), postprandial glucose response (6), the development of metabolic syndrome (7,8), and a myriad of diabetes complications (9). In addition, apoE4 carriers with diabetes have been shown to have increased carotid atherosclerosis (10), and elderly apoE4 carriers with diabetes have an increased risk of CVD-associated death (11).

Increases in VLDL TGs; decreases in HDL; the accumulation of smaller, more dense LDL; slower clearance of postprandial chylomicrons; and a decrease in LDL receptor (LDLR) expression are all noted phenotypes associated with both type 1 and type 2 diabetes (2). All of these components of diabetic dyslipidemia are areas of normal lipid metabolism in which apoE has previously been shown to play a direct role. The major receptor through which apoE mediates lipoprotein clearance is the LDLR, and the apoE isoforms exhibit differential LDLR binding affinities (12). Therefore, we sought whether apoE isoforms retain differential roles in diabetic dyslipidemia and atherosclerosis in the absence of the LDLR by using a mouse model of diabetes induced by streptozotocin (STZ).

In this study, we show that dyslipidemia and atherosclerosis are greatly exaggerated in diabetic $LDLR^{-/-}$ mice expressing human apoE4 ($E4LDLR^{-/-}$) compared with those with human apoE3 ($E3LDLR^{-/-}$), despite a similar degree of hyperglycemia. This E4-specific aggravation of diabetic dyslipidemia is central to the liver and is associated with a reduction in hepatic lipid oxidation, an accumulation of liver TGs, and increased rates of VLDL secretion.

RESEARCH DESIGN AND METHODS

Mice and induction of diabetes. Mice homozygous for replacement of the endogenous *Apoe* gene with the human *APOE*3* (E3) or *APOE*4* (E4) allele (13,14) were crossed with mice deficient in the LDLR (15). All mice were on C57BL/6 backgrounds. Male mice were fed normal chow diet ad libitum (5.3% fat and 0.02% cholesterol; Prolab IsoPro RMH 3000, Agway Inc., Syracuse, NY). Diabetes was induced at 2 months of age by peritoneal injections of STZ for 5 consecutive days (0.05 mg/g body wt in 0.05 mol/L citrate buffer, pH 4.5). Mice maintaining glucose levels >300 mg/dL throughout the course of the study are considered "diabetic." "Nondiabetic" control mice were injected with vehicle citrate buffer. Biochemical analyses were carried out at 1 month post-STZ unless otherwise stated. Animals were handled under protocols approved by the institutional animal care and use committees of the University of North Carolina.
Biochemical assays. After a 4-h fast, animals were anesthetized with 2,2,2-tribromoethanol and blood was collected. Plasma glucose, cholesterol, phospholipids, free fatty acids (FFAs), and ketone bodies were measured using

From the Department of Pathology and Laboratory Medicine, University of North Carolina at Chapel Hill, Chapel Hill, North Carolina.
Corresponding author: Nobuyo Maeda, nobuyo@med.unc.edu.
Received 7 April 2011 and accepted 29 June 2011.
DOI: 10.2337/db11-0466
This article contains Supplementary Data online at http://diabetes.diabetesjournals.org/lookup/suppl/doi:10.2337/db11-0466/-/DC1.

commercial kits (Wako, Richmond, VA). TGs and insulin were determined using commercial kits from Stanbio (Boerne, TX) and Crystal Chem Inc. (Downers Grove, IL), respectively. Liver TGs were extracted as described (16). Lipoprotein distribution and composition was determined with pooled (n = 6–8) plasma samples (100 μL) fractionated by fast-protein liquid chromatography using a Superose 6 HR10/30 column (GE Healthcare, Piscataway, NJ). Pooled plasma (800 μL) was separated by sequential density ultracentrifugation into density fractions from <1.006 g/mL (VLDL) to >1.21 g/mL (HDL) and subjected to electrophoresis in a 4–20% denaturing SDS-polyacrylamide gel (17). Carboxylmethyl lysine (CML) advanced glycation end products (AGEs) were measured using an enzyme-linked immunosorbent assay (ELISA) with antibodies specific for CML-AGEs (CycLex, Nagano, Japan). ApoE and apoCIII were measured using an ELISA with antibodies specific for apoE (Calbiochem, San Diego, CA) and apoCIII (Abcam, Cambridge, MA). Protein expression by Western blot was determined using antibodies against AMP-activated protein kinase (AMPK)-α, phosphorylated (Thr172) AMPK (pAMPK)-α, acetyl-CoA carboxylase (ACC), phosphorylated (Ser79) ACC (pACC), and β-actin (Cell Signaling, Boston, MA). Lipid tolerance test was performed by gavaging 10 mL/kg olive oil after an overnight fast. For VLDL secretion, plasma TG was measured after injection of Tyloxapol (Triton WR-1339, Sigma, St. Louis, MO) via tail vein (0.7 mg/g body wt) after a 4-h fast (18). VLDL lipolysis was estimated by incubating VLDL (25 μg TG in 60 μL PBS) at 37°C with 15 units of bovine lipoprotein lipase (Sigma). The reaction was stopped by adding 3 μL of 5 mol/L NaCl, and fatty acid release ($FA_{timepoint} - FA_0$) was measured as above.

Lipoprotein clearance. VLDL and LDL were labeled with 1,1′-Dioctadecyl-3,3,3′,3′-tetramethylindocarbocyanine iodide (DiI) or ^{125}I as previously described and injected to recipient mice via the tail vein (100 μg DiI-VLDL or 5×10^5 counts ^{125}I lipoproteins, diluted in 200 μL PBS) (18). Plasma fluorescence was measured using an Olympus FV500 (Texas Red filter) with a SPOT 2 digital camera. Radioactivity was counted on a Wallac 1470 Wizard γ Counter (EG&G Wallac, Gaithersburg, MD).

Lipid and glucose uptake, de novo lipogenesis, and oxidation. Primary hepatocytes were isolated from 3-month-old mice as described (19). Yield ranged from 3 to 6×10^6 cells/g liver and viability (assessed by Trypan blue staining) was >90%. After overnight culture in hepatocyte media (Xenotech, Lenexa, KS), cells (100,000/well, 24-well plate) were washed and cultured 72 h in Dulbecco's modified Eagle's medium supplemented with 5% FBS (volume for volume) with 5 mmol/L (low) or 25 mmol/L (high) glucose. Prior to dilution, [1-^{14}C]palmitic acid was resuspended in 1% BSA solution. For oxidation measurements, cells were incubated for 2 h with 1 μCi/mL D-[1-^{14}C]glucose or 1 μCi/mL [1-^{14}C]palmitic acid (PerkinElmer, Waltham, MA) while CO_2 was trapped using a customized 48-well NaOH trap (20). For 2-Deoxyglucose uptake, hepatocytes were starved in serum-free medium containing 135 mmol/L NaCl, 5.4 mmol/L KCl, 1.4 mmol/L CaCl2, 1.4 mmol/L MgSO4, and 10 mmol/L Na4P2O7 for 30 min and then incubated for 10 min with 1 μCi/mL 2-Deoxy-D [1-^{3}H]glucose (PerkinElmer). For fatty acid uptake and 2-Deoxyglucose uptake, cells were washed three times with ice-cold Hanks' balanced salt solution, lysed in 1 mL of 1% SDS, and radiation counted. To estimate de novo lipogenesis (DNL), cells were incubated with 1 μCi/mL D-[1-^{14}C]glucose for 24 h, washed three times with PBS, scraped in 1 mL of methanol-to-PBS (2:3), and freeze thawed in liquid nitrogen. The lipid layer was then extracted using a chloroform-to-methanol (2:1) extraction. Radiation was counted in 5 mL SX18–4 Scinteverse BD scintillation fluid (Fisher, Pittsburgh, PA) using an LKB Wallac 1214 RackBeta liquid scintillation counter (Spectrofuge, Durham, NC).

Indirect calorimetry. Mice were placed in a calorimetry system (LabMaster, TSE Systems, Chesterfield, MO) for 48 h and monitored for O_2 consumption, CO_2 production, and RQ (RQ = VCO_2/VO_2, where V is volume). Activity was determined by counting the number of breaks in light barriers on the X-, Y-, and Z-axis.

Atherosclerosis. After 3 months of diabetes, mice were killed with a lethal dose of 2,2,2-tribromoethanol and perfused at physiological pressure with 4% phosphate-buffered paraformaldehyde (pH 7.4). Morphometric analysis of plaque size at the aortic root was performed as described (19). Apoptotic cells were detected in 8-μm frozen sections of the aortic root with a kit that detects DNA fragmentation (Chemicon, Billerica, MA). Macrophages were detected with a 1:500 dilution of MOMA-2 (Abcam) and a 1:2,000 dilution of goat polyclonal secondary antibody to rat IgG - H&L Cy5 (Abcam).

RESULTS

Induction of diabetes. E3LDLR$^{-/-}$ and E4LDLR$^{-/-}$ mice had indistinguishable plasma glucose levels at the beginning and at the end of the study (Fig. 1*A* and Table 1). They showed a similar response rate to STZ, with 86.4 and 84.6% of injected E3LDLR$^{-/-}$ and E4LDLR$^{-/-}$ mice becoming diabetic. One month after STZ injection, average plasma glucose levels of E3LDLR$^{-/-}$ and E4LDLR$^{-/-}$ mice reached 424 ± 30 and 407 ± 44 mg/dL, respectively, and remained >400 mg/dL for the 3-month study period (Fig. 1*A* and Table 1). Plasma insulin levels in both genotypes dropped severely (Fig. 1*B*). The severity of diabetes was also comparable between the two diabetic groups as estimated by plasma levels of ketone bodies, daily food intake, and urine excretion (Table 1).

Diabetic dyslipidemia. Nondiabetic E3LDLR$^{-/-}$ and E4LDLR$^{-/-}$ mice had similar total plasma cholesterol and TGs (Fig. 2*A* and *B*) as well as similar lipoprotein distribution profiles (Fig. 2*C* and *D*). While the induction of diabetes led to increases in total cholesterol and total TGs in both E3LDLR$^{-/-}$ and E4LDLR$^{-/-}$ mice as early as 1 month after STZ administration, the increase in plasma cholesterol was significant only in E4LDLR$^{-/-}$ mice when compared with their nondiabetic counterparts. Most important, plasma cholesterol and TGs in the diabetic E4LDLR$^{-/-}$ mice were significantly higher than those in diabetic E3LDLR$^{-/-}$ mice at 1 and 3 months of diabetes (Fig. 2*A* and *B*).

VLDL and LDL cholesterol, as well as VLDL TGs, increased in both genotypes after STZ administration (Fig. 2*E* and *F*). However, VLDL TGs and LDL cholesterol were both twofold higher in E4LDLR$^{-/-}$ mice than in E3LDLR$^{-/-}$ mice (Fig. 2*E* and *F*). Consequently, the LDL-to-HDL ratio, an established risk factor for atherosclerosis, was 2.2-fold higher in diabetic E4LDLR$^{-/-}$ mice than in diabetic E3LDLR$^{-/-}$

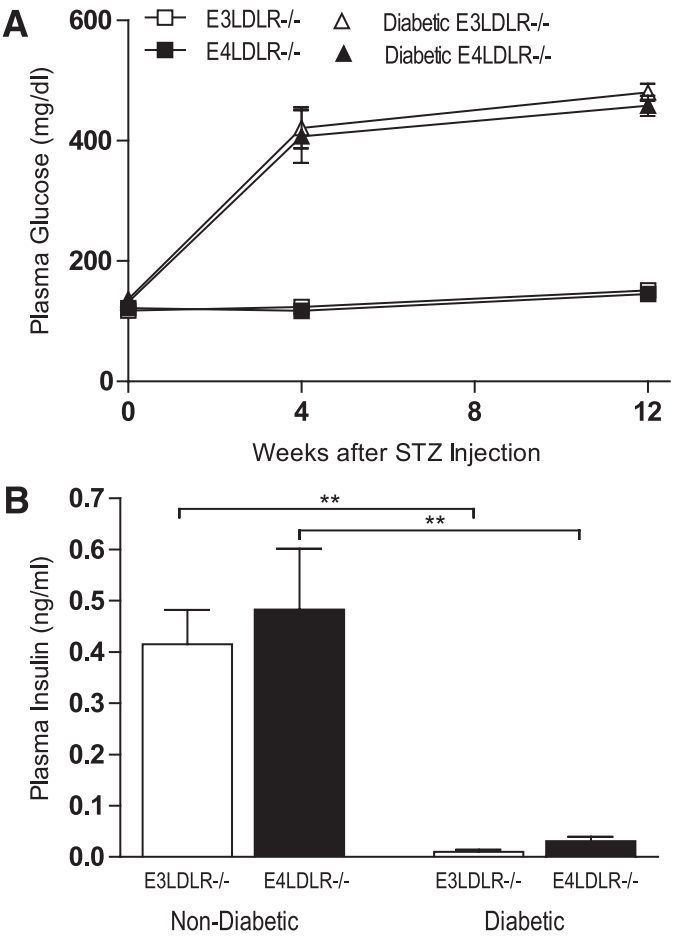

FIG. 1. Induction of diabetes. *A*: Fasting plasma glucose of nondiabetic E3LDLR$^{-/-}$ and nondiabetic E4LDLR$^{-/-}$ mice and after injection of STZ in diabetic E3LDLR$^{-/-}$ and diabetic E4LDLR$^{-/-}$ mice (n = 8–12 per group). *B*: Fasting plasma insulin, as determined by ELISA. **P < 0.01.

TABLE 1
Metabolic parameters of LDLR$^{-/-}$ mice expressing human apoE3 or apoE4

	E3LDLR$^{-/-}$	E4LDLR$^{-/-}$	Diabetic E3LDLR$^{-/-}$	Diabetic E4LDLR$^{-/-}$
Body weight (g)	29.5 ± 0.9	30.2 ± 1.3	23.9 ± 0.9†	24.6 ± 1.0†
Total cholesterol (mg/dL)	338.5 ± 14.4	372.4 ± 42.7	449.7 ± 46.7	795.9 ± 56.4*†
Total TGs (mg/dL)	296.9 ± 24.7	311.2 ± 26.5	431.8 ± 56.3	624.8 ± 48.1*†
FFAs (mmol/L)	0.92 ± 0.09	0.91 ± 0.10	1.16 ± 0.08	1.47 ± 0.05*†
Glucose (mg/dL)	146.3 ± 6.1	151.3 ± 4.9	470.8 ± 16.3†	479.3 ± 21.4†
Insulin (ng/mL)	0.42 ± 0.07	0.48 ± 0.12	0.01 ± 0.01†	0.03 ± 0.01†
Ketone bodies (μmol/L)	87.8 ± 27.4	122.5 ± 16.7	231.0 ± 43.9†	244.5 ± 49.7†
Lipoprotein AGEs (μg/mL)	2.02	1.95	2.30	2.38
Food consumed (g/day)#	4.8 ± 0.7	5.7 ± 1.1	11.9 ± 1.3†	12.6 ± 1.9†
Urine excretion (mL/day)#	2.0 ± 0.2	1.7 ± 0.2	13.8 ± 0.5†	13.6 ± 0.3†

Data are means ± SD. For the diabetic groups, measurements were taken 3 months after STZ administration (n = 8–18 per group). *$P > 0.05$, genotype effect. †$P > 0.05$, treatment effect. #n = 4–5 per group.

mice. Given that the diet provided was low in fat and cholesterol, food consumption did not differ between the two diabetic groups (Table 1); the enhanced hyperlipidemia in E4LDLR$^{-/-}$ is independent of dietary lipid intake.

VLDL fractionated from plasma by sequential ultracentrifugation had a similar composition of cholesterol, TGs, and phospholipids (Supplementary Fig. 1*A*). Diabetes induced a 5 and 26% increase in apoB100 and a 10 and 57% increase in apoB48 in E3LDLR$^{-/-}$ and E4LDLR$^{-/-}$ mice, respectively. Although total amounts of apoB100 and apoB48 are ~30% more in the diabetic E4LDLR$^{-/-}$ mice compared with diabetic E3LDLR$^{-/-}$ mice, their distributions among different classes of lipoproteins were not significantly altered (Supplementary Fig. 1*B–E*). In a similar manner, the amount of total plasma apoA1 did not differ by apoE genotype (Supplementary Fig. 1*F* and *G*). Diabetic E3LDLR$^{-/-}$ and diabetic E4LDLR$^{-/-}$ mice had similar lipoprotein distributions of apoE (Supplementary Fig. 2*A* and *B*) and apoCIII-to-apoE ratios, an important marker of lipolysis and uptake (Supplementary Fig. 2*C*). Rates of lipolysis were also similar between VLDL isolated from diabetic E3LDLR$^{-/-}$ or diabetic E4LDLR$^{-/-}$ mice (Supplementary Fig. 2*D*), suggesting similar rates of VLDL conversion between the two diabetic groups. In addition, the degree of glycation in the VLDL-LDL fractions was similar in all groups (Table 1).

In summary, diabetic E4LDLR$^{-/-}$ mice develop a far more deleterious plasma lipid and lipoprotein distribution profile than diabetic E3LDLR$^{-/-}$ mice, characterized by a substantial increase in the total amount of circulating lipoproteins, although not in the composition of the lipoprotein particles themselves.

Lipoprotein clearance and postprandial fat tolerance. As the model used lacks the LDLR, we measured the expression of several other genes involved in lipoprotein uptake. The expression of apoE, LDLR related protein 1 (LRP1), scavenger receptor B type 1 (SR-B1), and *N*-deacetylase/*N*-sulfotransferase 1 (NDST1) did not differ significantly between the two diabetic groups nor by induction of diabetes (Fig. 3*A*). Gene expression of VLDL receptor (VLDLR) was increased approximately eightfold by STZ administration, but the difference between diabetic E3LDLR$^{-/-}$ and E4LDLR$^{-/-}$ mice was not significant.

We next measured the efficiency of VLDL clearance in diabetic E3LDLR$^{-/-}$ and diabetic E4LDLR$^{-/-}$ mice by injecting VLDL isolated from apoE-deficient mice and labeled with DiI. There was no difference in the fractional catabolism of VLDL between the two diabetic groups (Fig. 3*B*). In a similar manner, there was no difference in the clearance of LDL particles isolated from nondiabetic LDLR$^{-/-}$ mice (Fig. 3*C*). We also examined whether the lipoprotein particles from diabetic mice with apoE3 or apoE4 are cleared differently by injecting nondiabetic LDLR$^{-/-}$ recipients of ^{125}I-labeled VLDL or LDL isolated from diabetic E3LDLR$^{-/-}$ or diabetic E4LDLR$^{-/-}$ mice. There was no difference in their clearance (Supplementary Fig. 3*A* and *B*). These data demonstrate that the clearance of VLDL remnants and LDL are not the major cause of the enhanced diabetic dyslipidemia observed in E4LDLR$^{-/-}$ mice compared with E3LDLR$^{-/-}$ mice.

Plasma TG levels in the diabetic E4LDLR$^{-/-}$ mice dropped to similar levels in E3LDLR$^{-/-}$ mice after an overnight fast. After administration of an oral gavage of olive oil to the diabetic mice, however, plasma TG levels of the E4LDLR$^{-/-}$ mice quickly reestablished a level twofold higher than E3LDLR$^{-/-}$ mice and remained high at all points postgavage (Fig. 3*D*). Except for the initial increase, clearance appeared to be equally impaired in the two groups, suggesting that diabetes is affecting postprandial lipid clearance equally. Intestinal absorption assessed by olive oil gavage after Tyloxapol injection did not differ by apoE genotype (Supplementary Fig. 4).

VLDL secretion. Altered hepatic VLDL secretion is a possible contributing factor to the elevated plasma lipids in the diabetic E4LDLR$^{-/-}$ mice. Thus, we measured plasma accumulation of TGs as a marker of VLDL secretion. After inhibition of VLDL uptake and lipolysis by injection of the detergent Tyloxapol, the TG secretion rate in nondiabetic E3LDLR$^{-/-}$ and E4LDLR$^{-/-}$ mice was similar, averaging 3.2 ± 0.5 and 4.0 ± 0.4 mg/dL/min TGs, respectively (Fig. 3*E*). The secretion rate in the diabetic E3LDLR$^{-/-}$ mice did not differ significantly from those of nondiabetic animals, averaging 3.5 ± 0.6 mg/dL/min TGs. In contrast, the secretion rate in the diabetic E4LDLR$^{-/-}$ mice was significantly elevated, averaging 7.0 ± 0.5 mg/dL/min and reaching a mean plasma TG level of 1,431.3 ± 49.3 mg/dL 2 h after Tyloxapol injection (Fig. 3*E*).

Energy usage, hepatic lipid stores, and fatty acid metabolism. To assess global energy metabolism in the diabetic E3LDLR$^{-/-}$ and E4LDLR$^{-/-}$ mice, indirect calorimetry analysis was performed. Diabetic E4LDLR$^{-/-}$ mice had significantly higher daily respiratory exchange ratios (RERs; V_{CO_2}/V_{O_2}), particularly during the light cycle, than E3LDLR$^{-/-}$ mice (Fig. 4*A* and *B*). This difference in RER was not because of altered activity (data not shown). A higher average RER in the diabetic LDLR$^{-/-}$ mice with E4

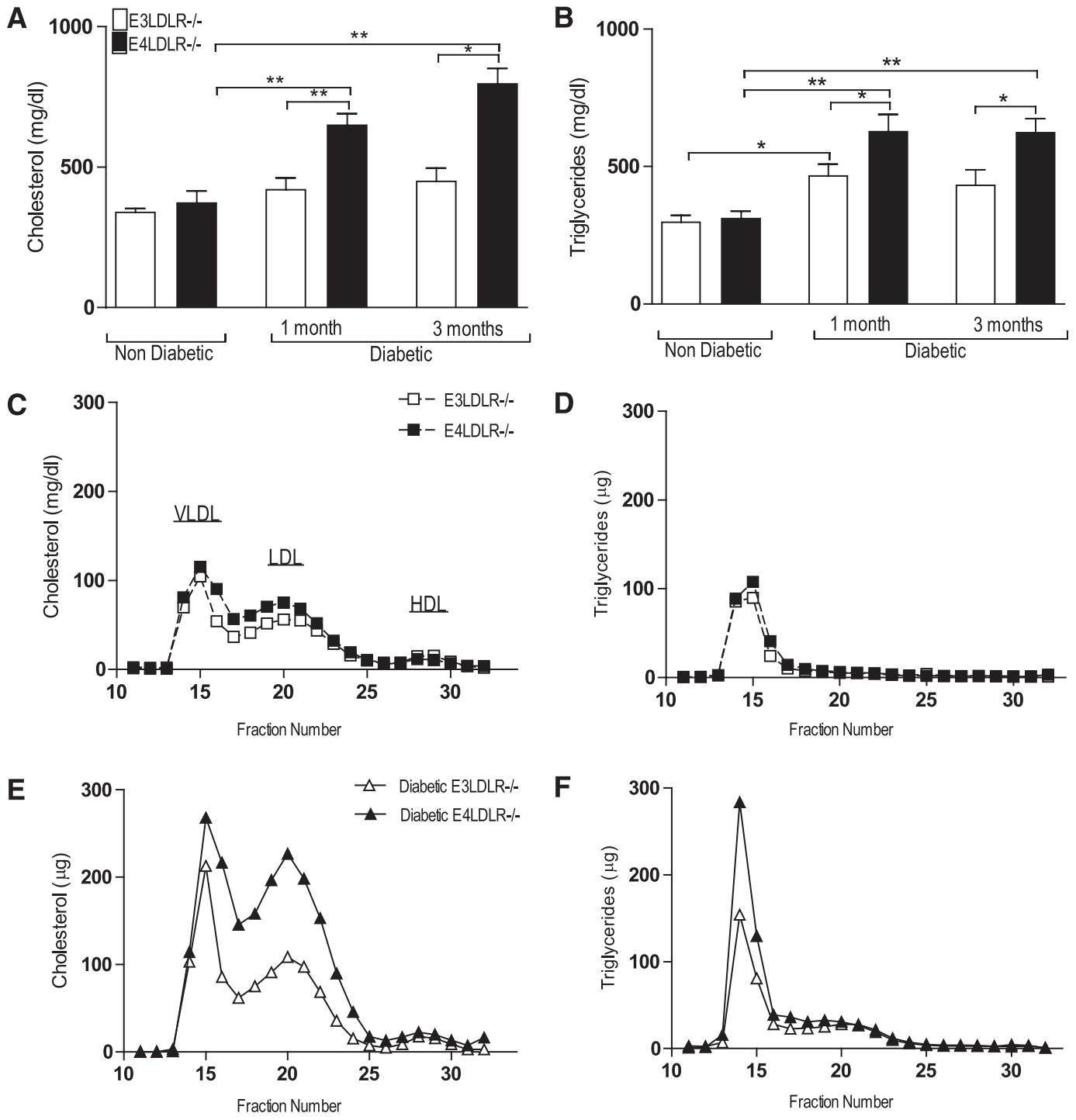

FIG. 2. Plasma lipids and lipoprotein profiles. *A* and *B*: Total plasma cholesterol (*A*) and TGs (*B*) after a 4-h fast (n = 8–18). *C* and *D*: Pooled (n = 6–8) plasma samples were separated into lipoprotein fractions by fast protein liquid chromatography. Lipoprotein cholesterol (*C*) and TG (*D*) profiles of nondiabetic E3LDLR$^{-/-}$ and nondiabetic E4LDLR$^{-/-}$ mice. *E* and *F*: Lipoprotein cholesterol (*E*) and TG (*F*) profiles of diabetic E3LDLR$^{-/-}$ and diabetic E4LDLR$^{-/-}$ mice. *$P < 0.05$ and **$P < 0.01$.

(0.915 ± 0.003) compared with those with E3 (0.896 ± 0.004, $P < 0.01$) during the light cycle indicates that the presence of apoE4 results in a lower fractional reliance on lipid as an energy source.

Nondiabetic E3LDLR$^{-/-}$ and E4LDLR$^{-/-}$ mice had similar TG stores in the liver. It is interesting that diabetes induced a significant accumulation of hepatic TGs only in E4LDLR$^{-/-}$ mice, because they store twice as much as diabetic E3LDLR$^{-/-}$ mice (Fig. 4*C*). This increase was not sufficient to cause overt steatosis, and there were no notable histological abnormalities in the livers of the diabetic mice (data not shown). The increase in hepatic TG storage in E4LDLR$^{-/-}$ mice during diabetes was also associated with an increase in plasma FFAs (Table 1).

Diabetes increased hepatic gene expression of SREBP1c and FOXO1, regulators of lipogenesis and VLDL secretion, respectively. Both tended to be higher in diabetic E4LDLR$^{-/-}$ mice compared with diabetic E3LDLR$^{-/-}$ mice, but the

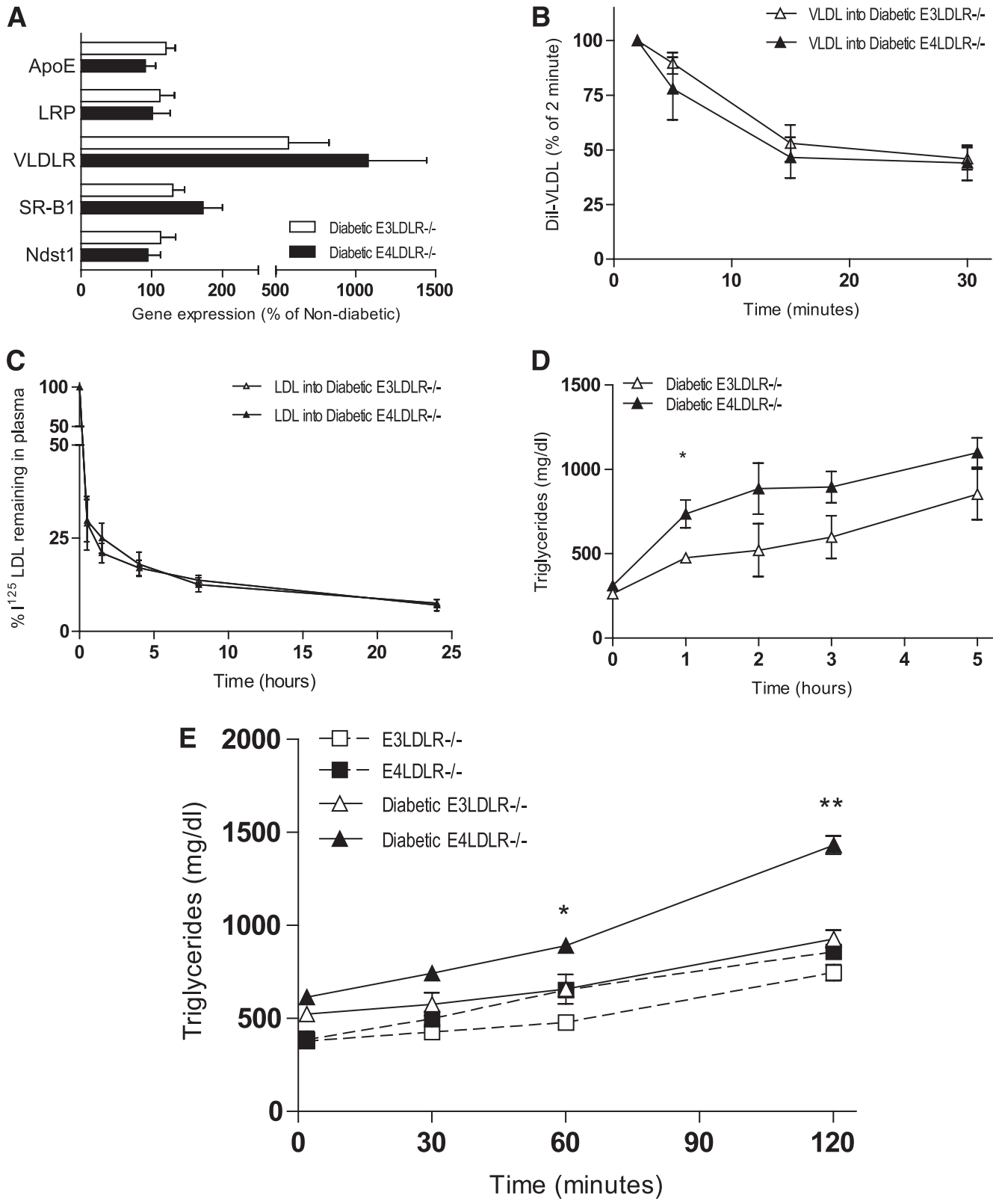

FIG. 3. Lipoprotein clearance and secretion. *A*: Liver mRNA levels of apoE, LRP, VLDLR, SR-B1, and NDST1. Data are expressed relative to nondiabetic mice (n = 6–7). *B* and *C*: Lipoprotein clearance. VLDL (*B*) and LDL (*C*) were isolated from plasma of APOE$^{-/-}$ mice and LDLR$^{-/-}$ mice, respectively, labeled with DiI, and injected into diabetic E3LDLR$^{-/-}$ and diabetic E4LDLR$^{-/-}$ mice after a 4-h fast. *D*: Postprandial lipid tolerance. Plasma TG was measured in diabetic E3LDLR$^{-/-}$ and diabetic E4LDLR$^{-/-}$ mice following an oral gavage of olive oil after overnight fast (n = 6–8). *E*: VLDL secretion. Plasma TGs of nondiabetic E3LDLR$^{-/-}$, nondiabetic E4LDLR$^{-/-}$, diabetic E3LDLR$^{-/-}$, and diabetic E4LDLR$^{-/-}$ mice after injection of Tyloxapol (n = 4–6 per group). *P < 0.05 and **P < 0.01.

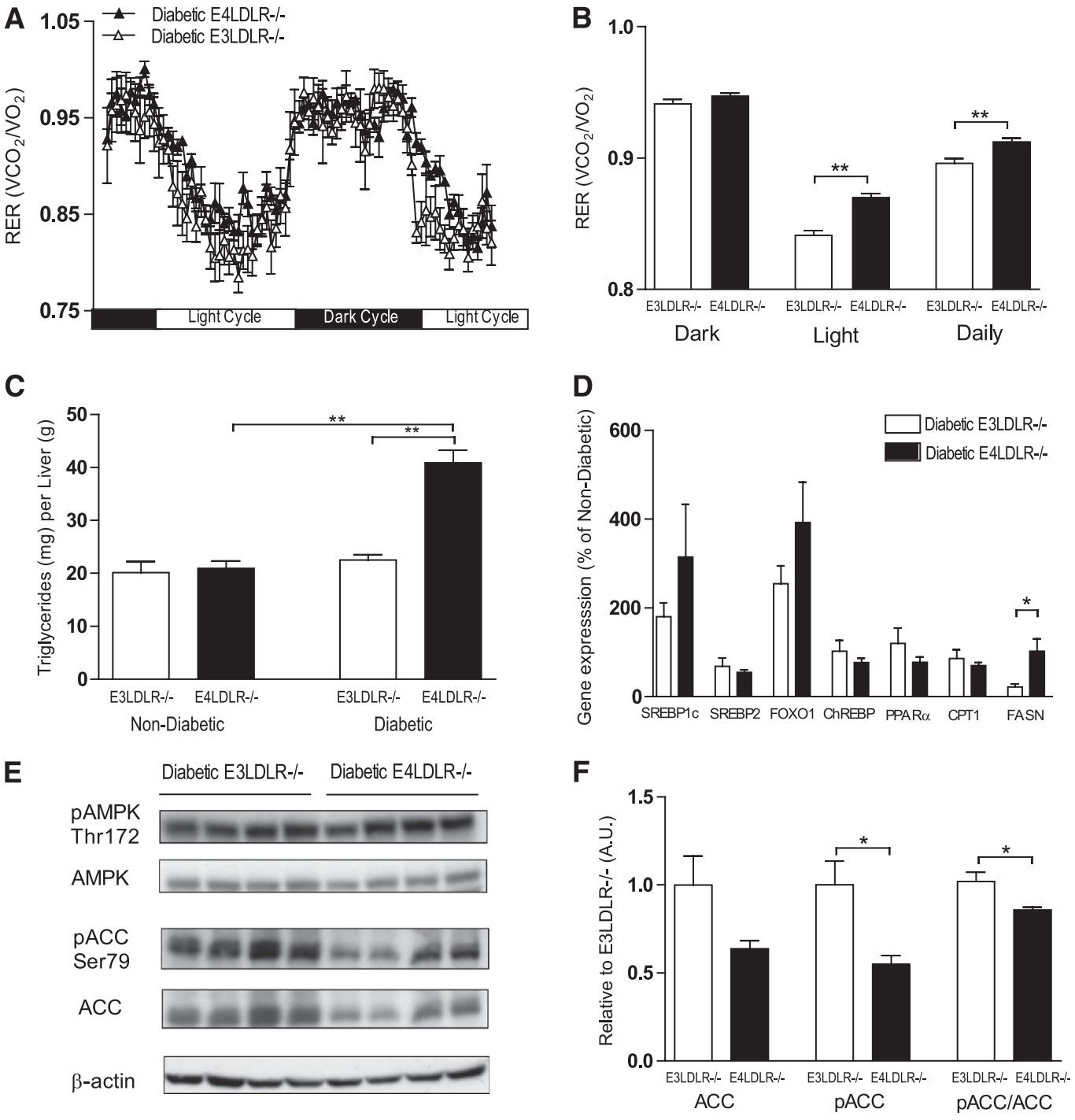

FIG. 4. Calorimetry, hepatic TG storage, and regulation of FA metabolism. *A* and *B*: RER (V_{CO_2}/V_{O_2}) was calculated over 48 h in diabetic E3LDLR$^{-/-}$ and diabetic E4LDLR$^{-/-}$ mice using indirect calorimetry (n = 4). *C*: Hepatic TG content. Liver TG was measured after homogenization and lipid extraction (n = 6–8). *D*: Gene expression of SREBP1c, SREBP2, FOXO1, ChREBP, PPARα, CPT1, and FASN in the livers of diabetic E3LDLR$^{-/-}$ and diabetic E4LDLR$^{-/-}$ mice. Data are expressed relative to nondiabetic mice (n = 8–14). *E*: Livers from diabetic E3LDLR$^{-/-}$ and diabetic E4LDLR$^{-/-}$ mice were homogenized and protein expression of pAMPK, total AMPK, pACC, and total ACC was determined by Western blot analysis (n = 4). *F*: Band intensity from *E* was quantitated using ImageJ software. Data are expressed relative to diabetic E3LDLR$^{-/-}$ in arbitrary units (AUs). *P < 0.05 and **P < 0.01.

increase did not reach significance (Fig. 4*D*). Expression of genes for SREBP2, ChREBP, PPAR-α, and CPT1 did not alter significantly between the two genotypes. It is important that expression of fatty acid synthase decreased significantly in E3LDLR$^{-/-}$ livers after STZ administration while remaining elevated in diabetic E4LDLR$^{-/-}$ livers (Fig. 4*D*). Although protein levels of AMPK and pAMPK were similar, a significantly lower pACC-to-ACC ratio was noted in livers isolated from diabetic E4LDLR$^{-/-}$ mice compared with E3LDLR$^{-/-}$ livers (Fig. 4*E* and *F*). Total ACC also tended to be lower but did not reach significance. A lower pACC-to-ACC ratio is indicative of decreased fatty acid oxidation and increased fatty acid synthesis. Together, these data suggest that increased fatty acid synthesis and reduced

fatty acid oxidation underlie an accumulation of lipid stores in the livers of diabetic E4LDLR$^{-/-}$ mice.

Glucose and lipid metabolism in primary hepatocytes. To verify a decrease in fatty acid oxidation in the livers of diabetic E4LDLR$^{-/-}$ mice, primary hepatocytes were isolated and cultured for 72 h in high (25 mmol/L) glucose medium to mimic the hyperglycemic environment of diabetes. Control cells were incubated in low glucose (5 mmol/L) for the same period. Similar to the TG accumulation noted in the liver in vivo, primary hepatocytes harvested from E4LDLR$^{-/-}$ mice and cultured in high glucose accumulated more lipid than E3LDLR$^{-/-}$ cells (Fig. 5*A* and *B*). The total area of lipid per cell was twofold higher in cells expressing E4 than E3 (16.6 ± 1.9 and 7.7 ± 0.6 μm^2/cell, respectively) (Fig. 5*B*).

FFA uptake, measured using [^{14}C]palmitic acid, increased in hepatocytes cultured in the high glucose medium but was not affected by apoE isoform (Fig. 5*C*). In a similar manner, there was no apoE isoform effect on the cellular uptake of glucose (Fig. 5*D*). The rate of DNL, defined here as ^{14}C incorporation into the lipid layer in cells cultured in the presence of [^{14}C]glucose, was higher in hepatocytes cultured in high glucose medium than those cultured in low glucose medium. However, hepatocytes isolated from E3LDLR$^{-/-}$and E4LDLR$^{-/-}$ mice did not differ in their rate of DNL in either the low or high glucose environment (Fig. 5*E*).

We next examined the rates of glucose and lipid oxidation in the E3LDLR$^{-/-}$ and E4LDLR$^{-/-}$ hepatocytes. Three days in high glucose medium decreased rates of [^{14}C]glucose oxidation in both E3LDLR$^{-/-}$ and E4LDLR$^{-/-}$ hepatocytes. However, there was no significant difference in glucose utilization between them (Fig. 5*F*). Finally, we measured lipid oxidation in primary hepatocytes cultured in high or low glucose using [^{14}C]palmitic acid. E3LDLR$^{-/-}$ and E4LDLR$^{-/-}$ hepatocytes cultured in the low glucose media demonstrated similar rates of lipid oxidation. When cultured in the high glucose environment, however, there was a striking downregulation of lipid oxidation only in E4LDLR$^{-/-}$ hepatocytes (Fig. 5*G*). After 72 h in the high glucose condition, the E4LDLR$^{-/-}$ hepatocytes had lipid oxidation rates ~40% of those in the E3LDLR$^{-/-}$ hepatocytes.

Diabetic atherosclerosis. Reflecting their severe dyslipidemia, diabetic LDLR$^{-/-}$ mice carrying the E4 allele had aortic plaques on average threefold greater in area than those with E3 (Fig. 6). The size of the atherosclerotic plaques in diabetic E4LDLR$^{-/-}$ mice (141,000 ± 19,000 μm^2) was significantly greater when compared with diabetic E3LDLR$^{-/-}$ mice (48,000 ± 9,000 μm^2) as well as to both nondiabetic E3LDLR$^{-/-}$ and nondiabetic E4LDLR$^{-/-}$ mice (32,000 ± 8,000 and 40,000 ± 12,000 μm^2) (Fig. 6). While diabetic E4LDLR$^{-/-}$ mice had larger and more complex atherosclerotic lesions than diabetic E3LDLR$^{-/-}$ mice, the number of macrophages (Supplementary Fig. 5*A* and *B*) and apoptotic cells (Supplementary Fig. 5*C* and *D*) per lesion area were similar between the two groups.

DISCUSSION

In the present work, we explored the isoform-specific role of apoE in diabetic dyslipidemia using diabetic LDLR$^{-/-}$ mice with human apoE4 or apoE3. We found that *1*) nondiabetic E3LDLR$^{-/-}$ and E4LDLR$^{-/-}$ mice are indistinguishable in all parameters of glucose and lipid metabolism measured in this study; *2*) after induction of diabetes, E4LDLR$^{-/-}$ mice, but not E3LDLR$^{-/-}$, develop enhanced dyslipidemia, characterized by elevated VLDL TG and LDL cholesterol, and an increased rate of VLDL secretion; *3*) the severe dyslipidemia in diabetic E4LDLR$^{-/-}$ mice is associated with larger hepatic lipid stores and a calorimetric profile suggestive of lower lipid utilization; *4*) primary hepatocytes isolated from E4LDLR$^{-/-}$ mice and cultured in high glucose accumulated more intracellular lipid concomitant with a reduction in fatty acid oxidation; and *5*) these metabolic disturbances during diabetes culminated in exaggerated atherosclerosis only in E4LDLR$^{-/-}$ mice.

Diabetic dyslipidemia in poorly treated type 1 diabetes and type 2 diabetes shares many features (2). In many patients with diabetes, the levels of circulating lipoproteins during fasting are relatively normal (21). Instead, the major impairments to lipoprotein metabolism occur with their ability to clear postprandial lipoproteins (2). The prolonged elevation of plasma TGs after a fatty meal has been demonstrated in individuals carrying the E4 allele (6), and our previous work demonstrated postprandial lipemia in LDLR overexpressing mice with human apoE4 (22). Previously, Goldberg et al. (23) showed that STZ-induced diabetic LDLR$^{-/-}$ mice accumulated a "subclass of lipoproteins" that normally is quickly removed from the circulation. Our experiments confirmed that postprandial lipid clearance is impaired in diabetic LDLR$^{-/-}$ mice. However, except for initial increase in plasma TG in E4LDLR$^{-/-}$ mice, the postprandial clearance rate was not different in two groups. In addition, we found no APOE genotype effect on the fractional catabolism of either VLDL or LDL.

VLDL production is increased in type 2 diabetes and in uncontrolled type 1 diabetes (2). In insulin-resistant patients, this increased VLDL production is oftentimes part of a dyslipidemic cycle in which larger adipose tissue stores are associated with increased FFA release (24). In turn, an increased flux of FFA to the liver stimulates VLDL secretion (25). The FFA-stimulated VLDL production is compounded in an insulin-resistant or insulin-deficient state (2). Along these lines, the increased plasma VLDL in the diabetic E4LDLR$^{-/-}$ mice is accompanied by a twofold increase in TG secretion. In comparison, TG secretion in the diabetic E3LDLR$^{-/-}$ mice was not different from that in the nondiabetic controls. In a similar manner, LDLR$^{-/-}$ mice expressing murine apoE do not have increased rates of TG production after STZ-induced diabetes (23). We note that increased hepatic secretion of TG-rich particles is most likely responsible for the majority of LDL-sized particles in E4LDLR$^{-/-}$ mice, since absence of LDLR has been shown to result in overproduction of TG-rich particles smaller than normal VLDL (26,27). Thus, the dyslipidemic cycle commonly seen in patients with insulin resistance is reflected by the insulin-deficient E4LDLR$^{-/-}$ mice used in this study, which have higher circulating FFA, larger hepatic TG stores, and higher rates of TG secretion than diabetic E3LDLR$^{-/-}$ mice.

Indirect calorimetry analysis revealed a clear apoE genotype effect on energy usage during diabetes at the whole body level. Diabetic E4LDLR$^{-/-}$ mice had significantly higher RER, demonstrating a lower ratio of lipid-to-carbohydrate oxidation compared with diabetic E3LDLR$^{-/-}$ mice during the light cycle. This reduced reliance on lipid oxidation appears to be central to the liver and directed by ACC signaling. When active, ACC catalyzes the production of malonyl-CoA, thereby stimulating lipogenesis and inhibiting the β-oxidation of fatty acids (28). A significant reduction in the pACC-to-ACC ratio in the livers of diabetic E4LDLR$^{-/-}$ mice indicates an increase in lipogenesis and

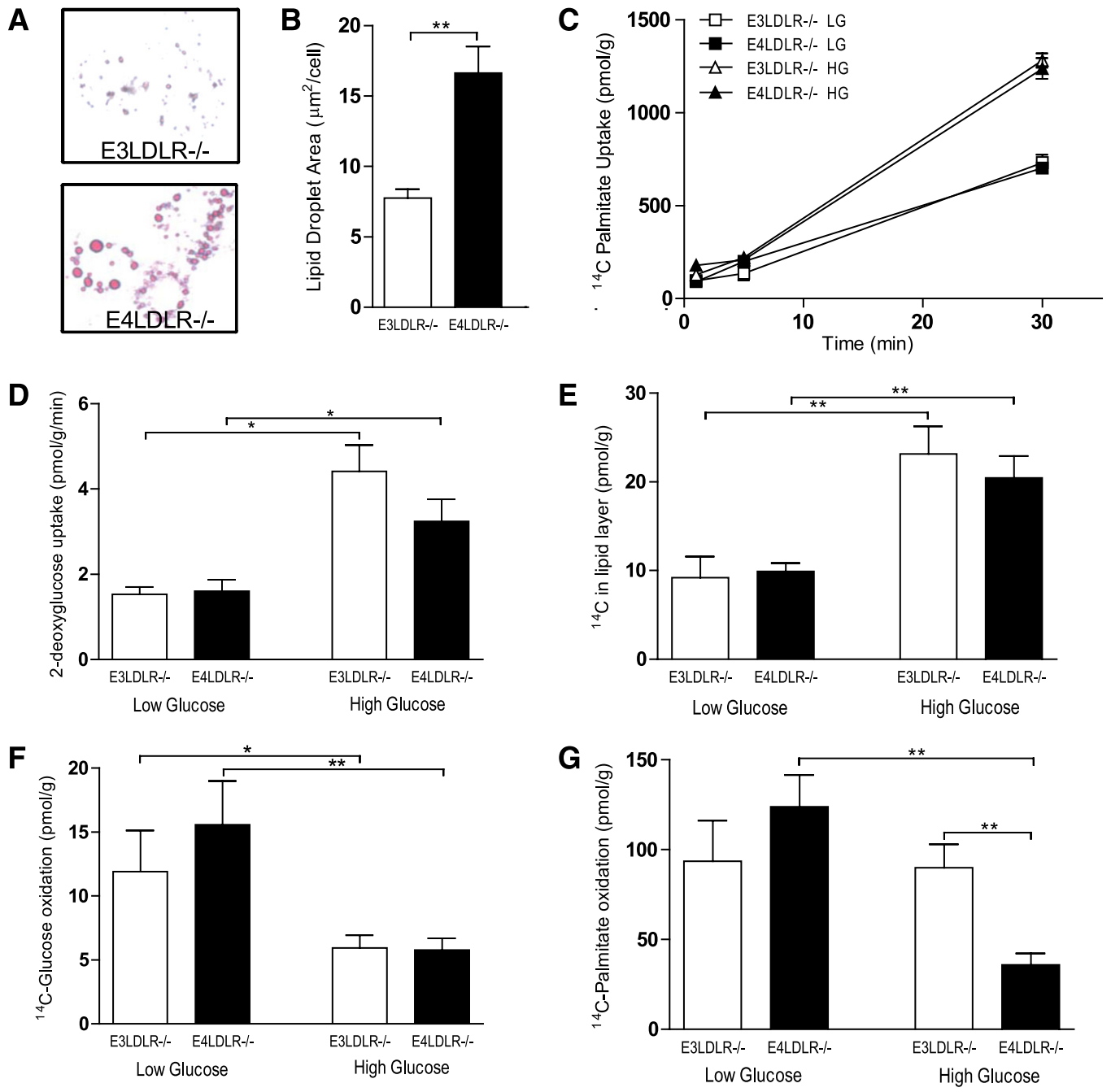

FIG. 5. Metabolic analyses of primary hepatocytes. *A*: Primary hepatocytes from E3LDLR$^{-/-}$ or E4LDLR$^{-/-}$ mice were cultured for 72 h in high glucose (25 mmol/L) media and stained with Oil Red O to highlight lipid droplets. *B*: Total lipid droplet area per cell was quantified by measuring 50 randomly chosen cells from four separate cultures per group. *C*: Fatty acid uptake was estimated by counting intracellular radiation after incubating hepatocytes for 1 min with 2 μCi/mL [^{14}C]palmitate. *D*: Glucose uptake was measured after a 10-min incubation with 1 μCi/mL ^{3}H-2-deoxyglucose after starving cells for 2 h. *E*: DNL was measured by counting radiation in the lipid layer after 24-h incubation with [^{14}C]glucose. *F* and *G*: Oxidation of [^{14}C]glucose (*F*) and [^{14}C]palmitate (*G*) was measured by trapping $^{14}CO_2$ during a 3-h incubation using a customized, self-contained CO_2 trap (n = 4–12 wells per trial, three trials per group). *$P < 0.05$ and **$P < 0.01$. (A high-quality color representation of this figure is available in the online issue.)

decrease in fatty acid oxidation. In addition, STZ administration decreased *FASN* gene expression in the E3LDLR$^{-/-}$ mice, as previously reported in wild-type mice (29). However, this diabetes-induced reduction did not occur in E4LDLR$^{-/-}$ mice, suggesting a higher rate of fatty acid synthesis in these mice. Higher expression of *FASN* was not the result of stimulation by *ChREBP*. Expression of *SREBP1c*, an important regulator of *FASN*-directed lipogenesis, on the other hand, tended to be higher in the diabetic E4LDLR$^{-/-}$ livers but did not reach significance. Regardless, these data point toward two distinct means (metabolically linked by ACC signaling) by which lipid accumulates in the E4LDLR$^{-/-}$ livers during diabetes—an increase in fatty acid synthesis and a reduction in fatty acid oxidation. Consistent with these data, apoE4-expressing LDLR$^{-/-}$ hepatocytes cultured in high glucose reduced their rate of lipid oxidation to levels ~40% of that in E3LDLR$^{-/-}$ hepatocytes and amassed more than twice as much lipid.

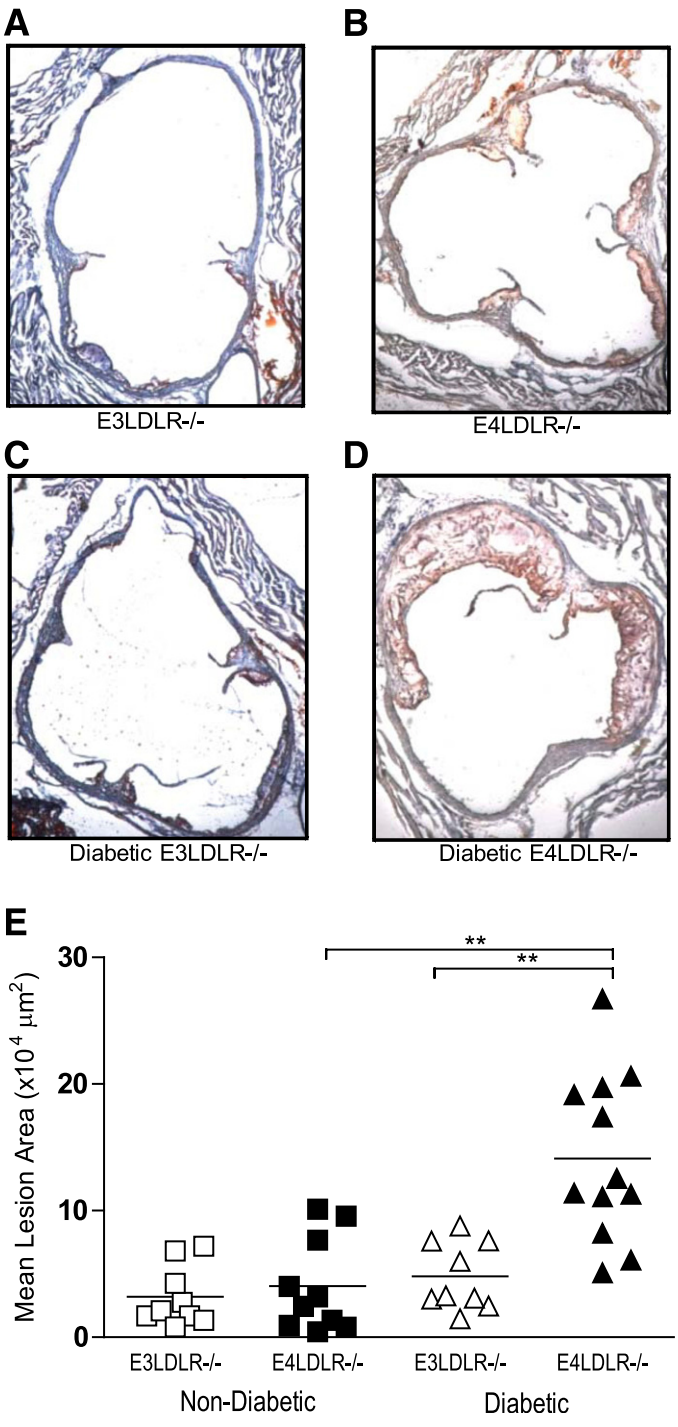

FIG. 6. Atherosclerosis at the aortic root. *A–D*: Cross sections of the aortic root were stained with hematoxylin-eosin and Oil Red O. Photos are representative of the mean plaque size of nondiabetic E3LDLR$^{-/-}$ (*A*), nondiabetic E4LDLR$^{-/-}$ (*B*), diabetic E3LDLR$^{-/-}$ (*C*), and diabetic E4LDLR$^{-/-}$ mice (*D*). *E*: Data points represent the average lesion area of four distinct histological sections of the aortic root (n = 9–12 per group). **$P < 0.01$. (A high-quality digital representation of this figure is available in the online issue.)

LDLR$^{-/-}$ mice are an established model for high-fat diet–induced obesity and insulin resistance, and we have previously shown that mice expressing apoE4 are more susceptible to diet-induced glucose intolerance than those expressing apoE3 (30). This propensity of apoE4-expressing mice to develop glucose intolerance likely contributes to the impaired lipid metabolism in the insulin-deficient state. In this context, we note that VLDLR mRNA was significantly increased after the STZ administration, and the mRNA levels tended to be higher in the diabetic E4LDLR$^{-/-}$ livers than in the diabetic E3LDLR$^{-/-}$ livers. While the contribution of VLDLR in hepatic remnant clearance during diabetes is not clear, fasting hypertriglyceridemia in VLDLR$^{-/-}$ mice has been previously noted (31), and when overexpressed in the liver, VLDLR appears to function similarly to LDLR and LRP (32). The VLDLR plays an important role in adipocyte TG accumulation (33) and could be a potential player in the process of hepatic lipid accumulation during diabetes.

Our results support the possibility that apoE functions as a metabolic signaling molecule outside its established role in lipoprotein clearance. For example, a role for apoE as a signaling molecule has been shown previously in the context of Alzheimer disease (34), where it has been shown to affect activation of extracellular signal-regulated kinase 1/2 and c-Jun NH_2-terminal kinase in an apoE isoform–specific manner (35). Similar apoE4-specific signaling could account for some of the metabolic abnormalities during diabetes highlighted in this study. Alternatively, apoE has been shown to enhance VLDL secretion (36), as well as play a role in the accumulation of lipid in early and intermediary secretory compartments of hepatocytes (37). Thus, inefficient recycling and resecretion of apoE4 (38) could potentially affect the availability, packaging, and/or transport of TG from the hepatic lipid pool. Irrespective of the precise mode of action, our results demonstrate a possible chain of events in diabetic E4LDLR$^{-/-}$ livers; a downregulation of lipid oxidation and upregulation of fatty acid synthesis lead to larger hepatic TG stores, which in turn drive an increase in VLDL secretion. Combined with marked diabetic effects that impair VLDL and postprandial TG clearance, these processes are ultimately responsible for the severe dyslipidemia observed in the diabetic E4LDLR$^{-/-}$ mice.

It is important that the diabetes-induced acceleration of atherosclerosis occurs only in LDLR$^{-/-}$ mice expressing apoE4. Previous studies of STZ-induced diabetes in LDLR$^{-/-}$ mice have produced variable results, with some groups showing an increase in atherosclerosis (39,40) while others show no change (41,42). Although the reasons for these mixed results are unknown, varying experimental conditions, such as diet, could contribute (43). The E4-specific acceleration of atherosclerosis is likely a direct result of the severe dyslipidemia brought about by STZ-induced diabetes in these mice, although contributions of other factors, such as apoE4-specific effects on macrophages, cannot be excluded (44). Regardless, our data clearly demonstrate the presence of E4 effects that are independent of the LDLR. Moreover, the exaggerated dyslipidemia and atherosclerosis observed in the diabetic E4LDLR$^{-/-}$ mice extends beyond the scope of type 1 diabetes and has implications for the growing number of apoE4 carriers with insulin resistance and type 2 diabetes. In conclusion, the apoE4-specific atherosclerosis and diabetic dyslipidemia illustrated in this study may also play an important role in patients with diabetes who carry the apoE4 isoform.

ACKNOWLEDGMENTS

L.A.J. has received an American Heart Association Predoctoral Fellowship (10PRE3880032). R.G.F. has received

an American Heart Association Predoctoral Fellowship (T32 HL69768). N.M. has received grants from the National Institutes of Health (HL-42630 and HL-087946).

No potential conflicts of interest relevant to this article were reported.

L.A.J. designed and performed the experiments and wrote the manuscript. J.M.A.-M., R.G.F, A.A.P., M.K.A., and H.-S.K. performed the experiments. N.M. designed the overall study and wrote the manuscript.

The authors thank Marcus McNair, Shinja Kim, Sabrina Baxter, Melissa Knudson, Taylor Nipp, and Kunjie Hua of the University of North Carolina at Chapel Hill for technical assistance.

REFERENCES

1. Grundy SM, Benjamin IJ, Burke GL, et al. Diabetes and cardiovascular disease: a statement for healthcare professionals from the American Heart Association. Circulation 1999;100:1134–1146
2. Goldberg IJ. Clinical review 124: Diabetic dyslipidemia: causes and consequences. J Clin Endocrinol Metab 2001;86:965–971
3. Mahley RW, Rall SC Jr. Apolipoprotein E: far more than a lipid transport protein. Annu Rev Genomics Hum Genet 2000;1:507–537
4. Scuteri A, Najjar SS, Muller D, et al. apoE4 allele and the natural history of cardiovascular risk factors. Am J Physiol Endocrinol Metab 2005;289: E322–E327
5. Elosua R, Demissie S, Cupples LA, et al. Obesity modulates the association among APOE genotype, insulin, and glucose in men. Obes Res 2003;11: 1502–1508
6. Dart A, Sherrard B, Simpson H. Influence of apo E phenotype on postprandial triglyceride and glucose responses in subjects with and without coronary heart disease. Atherosclerosis 1997;130:161–170
7. Sima A, Iordan A, Stancu C. Apolipoprotein E polymorphism—a risk factor for metabolic syndrome. Clin Chem Lab Med 2007;45:1149–1153
8. Olivieri O, Martinelli N, Bassi A, et al. ApoE epsilon2/epsilon3/epsilon4 polymorphism, ApoC-III/ApoE ratio and metabolic syndrome. Clin Exp Med 2007;7:164–172
9. Freedman BI, Bostrom M, Daeihagh P, Bowden DW. Genetic factors in diabetic nephropathy. Clin J Am Soc Nephrol 2007;2:1306–1316
10. Elosua R, Ordovas JM, Cupples LA, et al. Association of APOE genotype with carotid atherosclerosis in men and women: the Framingham Heart Study. J Lipid Res 2004;45:1868–1875
11. Guang-da X, You-ying L, Zhi-song C, Yu-sheng H, Xiang-jiu Y. Apolipoprotein e4 allele is predictor of coronary artery disease death in elderly patients with type 2 diabetes mellitus. Atherosclerosis 2004;175:77–81
12. Weisgraber KH. Apolipoprotein E: structure-function relationships. Adv Protein Chem 1994;45:249–302
13. Sullivan PM, Mezdour H, Aratani Y, et al. Targeted replacement of the mouse apolipoprotein E gene with the common human APOE3 allele enhances diet-induced hypercholesterolemia and atherosclerosis. J Biol Chem 1997;272:17972–17980
14. Knouff C, Hinsdale ME, Mezdour H, et al. Apo E structure determines VLDL clearance and atherosclerosis risk in mice. J Clin Invest 1999;103: 1579–1586
15. Knouff C, Briand O, Lestavel S, Clavey V, Altenburg M, Maeda N. Defective VLDL metabolism and severe atherosclerosis in mice expressing human apolipoprotein E isoforms but lacking the LDL receptor. Biochim Biophys Acta 2004;1684:8–17
16. Folch J, Lees M, Sloane Stanley GH. A simple method for the isolation and purification of total lipides from animal tissues. J Biol Chem 1957;226:497–509
17. de Silva HV, Más-Oliva J, Taylor JM, Mahley RW. Identification of apolipoprotein B-100 low density lipoproteins, apolipoprotein B-48 remnants, and apolipoprotein E-rich high density lipoproteins in the mouse. J Lipid Res 1994;35:1297–1310
18. Johnson LA, Altenburg MK, Walzem RL, Scanga LT, Maeda N. Absence of hyperlipidemia in LDL receptor-deficient mice having apolipoprotein B100 without the putative receptor-binding sequences. Arterioscler Thromb Vasc Biol 2008;28:1745–1752
19. Altenburg M, Arbones-Mainar J, Johnson L, Wilder J, Maeda N. Human LDL receptor enhances sequestration of ApoE4 and VLDL remnants on the surface of hepatocytes but not their internalization in mice. Arterioscler Thromb Vasc Biol 2008;28:1104–1110
20. Wang X, Wang R, Nemcek TA, Cao N, Pan JY, Frevert EU. A self-contained 48-well fatty acid oxidation assay. Assay Drug Dev Technol 2004;2:63–69
21. Ginsberg HN. Lipoprotein physiology in nondiabetic and diabetic states. Relationship to atherogenesis. Diabetes Care 1991;14:839–855
22. Malloy SI, Altenburg MK, Knouff C, Lanningham-Foster L, Parks JS, Maeda N. Harmful effects of increased LDLR expression in mice with human APOE*4 but not APOE*3. Arterioscler Thromb Vasc Biol 2004;24:91–97
23. Goldberg IJ, Hu Y, Noh HL, et al. Decreased lipoprotein clearance is responsible for increased cholesterol in LDL receptor knockout mice with streptozotocin-induced diabetes. Diabetes 2008;57:1674–1682
24. Lewis GF. Fatty acid regulation of very low density lipoprotein production. Curr Opin Lipidol 1997;8:146–153
25. Adiels M, Taskinen MR, Packard C, et al. Overproduction of large VLDL particles is driven by increased liver fat content in man. Diabetologia 2006; 49:755–765
26. Twisk J, Gillian-Daniel DL, Tebon A, Wang L, Barrett PH, Attie AD. The role of the LDL receptor in apolipoprotein B secretion. J Clin Invest 2000; 105:521–532
27. Nassir F, Xie Y, Patterson BW, Luo J, Davidson NO. Hepatic secretion of small lipoprotein particles in apobec-1-/- mice is regulated by the LDL receptor. J Lipid Res 2004;45:1649–1659
28. Brownsey RW, Boone AN, Elliott JE, Kulpa JE, Lee WM. Regulation of acetyl-CoA carboxylase. Biochem Soc Trans 2006;34:223–227
29. Jourdan T, Djaouti L, Demizieux L, Gresti J, Vergès B, Degrace P. Liver carbohydrate and lipid metabolism of insulin-deficient mice is altered by trans-10, cis-12 conjugated linoleic acid. J Nutr 2009;139:1901–1907
30. Arbones-Mainar JM, Johnson LA, Altenburg MK, Maeda N. Differential modulation of diet-induced obesity and adipocyte functionality by human apolipoprotein E3 and E4 in mice. Int J Obes (Lond) 2008;32:1595–1605
31. Yagyu H, Lutz EP, Kako Y, et al. Very low density lipoprotein (VLDL) receptor-deficient mice have reduced lipoprotein lipase activity. Possible causes of hypertriglyceridemia and reduced body mass with VLDL receptor deficiency. J Biol Chem 2002;277:10037–10043
32. Kobayashi K, Oka K, Forte T, et al. Reversal of hypercholesterolemia in low density lipoprotein receptor knockout mice by adenovirus-mediated gene transfer of the very low density lipoprotein receptor. J Biol Chem 1996;271:6852–6860
33. Goudriaan JR, Tacken PJ, Dahlmans VE, et al. Protection from obesity in mice lacking the VLDL receptor. Arterioscler Thromb Vasc Biol 2001;21: 1488–1493
34. Hoe HS, Harris DC, Rebeck GW. Multiple pathways of apolipoprotein E signaling in primary neurons. J Neurochem 2005;93:145–155
35. Korwek KM, Trotter JH, Ladu MJ, Sullivan PM, Weeber EJ. ApoE isoform-dependent changes in hippocampal synaptic function. Mol Neurodegener 2009;4:21
36. Huang Y, Liu XQ, Rall SC Jr, et al. Overexpression and accumulation of apolipoprotein E as a cause of hypertriglyceridemia. J Biol Chem 1998;273: 26388–26393
37. Mensenkamp AR, Van Luyn MJ, Havinga R, et al. The transport of triglycerides through the secretory pathway of hepatocytes is impaired in apolipoprotein E deficient mice. J Hepatol 2004;40:599–606
38. Heeren J, Beisiegel U, Grewal T. Apolipoprotein E recycling: implications for dyslipidemia and atherosclerosis. Arterioscler Thromb Vasc Biol 2006; 26:442–448
39. Keren P, George J, Shaish A, et al. Effect of hyperglycemia and hyperlipidemia on atherosclerosis in LDL receptor-deficient mice: establishment of a combined model and association with heat shock protein 65 immunity. Diabetes 2000;49:1064–1069
40. Renard CB, Kramer F, Johansson F, et al. Diabetes and diabetes-associated lipid abnormalities have distinct effects on initiation and progression of atherosclerotic lesions. J Clin Invest 2004;114:659–668
41. Berti JA, Salerno AG, Bighetti EJ, Casquero AC, Boschero AC, Oliveira HC. Effects of diabetes and CETP expression on diet-induced atherosclerosis in LDL receptor-deficient mice. APMIS 2005;113:37–44
42. Reaven P, Merat S, Casanada F, Sutphin M, Palinski W. Effect of streptozotocin-induced hyperglycemia on lipid profiles, formation of advanced glycation endproducts in lesions, and extent of atherosclerosis in LDL receptor-deficient mice. Arterioscler Thromb Vasc Biol 1997;17:2250–2256
43. Johnson LA, Maeda N. Macrovascular complications of diabetes in atherosclerosis prone mice. Expert Rev Endocrinol Metab 2010;5:89–98
44. Altenburg M, Johnson L, Wilder J, Maeda N. Apolipoprotein E4 in macrophages enhances atherogenesis in a low density lipoprotein receptor-dependent manner. J Biol Chem 2007;282:7817–7824